Acta Crystallographica Section D
Biological Crystallography
ISSN 0907-4449

Separation and crystallization of $T = 3$ and $T = 4$ icosahedral complexes of the hepatitis B virus core protein

Adam Zlotnick,[a] Ira Palmer,[a] Joshua D. Kaufman,[a] Stephen J. Stahl,[a] Alasdair C. Steven[b] and Paul T. Wingfield[a]*

[a]Protein Expression Laboratory, National Institute of Arthritis, Musculoskeletal and Skin Diseases, National Institutes of Health, Bethesda, MD 20892, USA, and [b]Laboratory of Structural Biology, National Institute of Arthritis, Musculoskeletal and Skin Diseases, National Institutes of Health, Bethesda, MD 20892, USA

Correspondence e-mail: pelpw@helix.nih.gov

Received 10 June 1998
Accepted 15 October 1998

The icosahedral nucleocapsid of human hepatitis B virus is a homopolymer of the dimeric capsid protein also known as hepatitis B core antigen or HBcAg. Purified capsid protein obtained from an *Escherichia coli* expression system was reassembled into a mixture of $T = 3$ and $T = 4$ icosahedral particles consisting of 90 and 120 dimers, respectively. The two types of capsid were separated on a preparative scale by centrifugation through a sucrose gradient. In addition to this heterogeneity, the capsid protein has three cysteines, one of which has a great propensity for forming disulfide bonds between the two subunits, forming a dimer. To eliminate heterogeneity arising from oxidation, alanines were substituted for the cysteines. $T = 3$ and $T = 4$ capsids crystallized under similar conditions. Crystals of $T = 3$ capsids diffracted to ~8 Å resolution; crystals of $T = 4$ capsids diffracted to 4 Å resolution.

1. Introduction

Hepatitis B virus (HBV), a prevalent human liver pathogen which can lead to cirrhosis and/or hepatocellular carcinoma (Blumberg, 1997), is an enveloped DNA virus with an RNA intermediate (Summers & Mason, 1982). *In vivo*, virus assembly is initiated by formation of a protein capsid around a complex of the viral reverse transcriptase and viral mRNA (Bartenschlager & Schaller, 1992).

The capsid protein is a 183-residue protein which can be isolated as a homodimer (Wingfield *et al.*, 1995). The first 149 residues form an assembly domain (Birnbaum & Nassal, 1990). The C-terminal 34 residues form the protamine domain which is required for nucleic acid packaging but not for capsid assembly (Milich *et al.*, 1988). Full-length capsid protein and assembly domain have been expressed in *Escherichia coli*, where they form capsids (Pasek *et al.*, 1979; Stahl *et al.*, 1982; Cohen & Richmond, 1982).

Two different sizes of icosahedral capsid are found in authentic HBV from infected human liver (Kenney *et al.*, 1995), recombinant capsids from *E. coli* (Crowther *et al.*, 1994) and *in vitro* assembled recombinant capsid protein (Wingfield *et al.*, 1995); the biological role of the two forms is unknown. Image reconstructions (see Fig. 1) derived from cryo-electron microscopy data have revealed many features of the two forms (Crowther *et al.*, 1994; Kenney

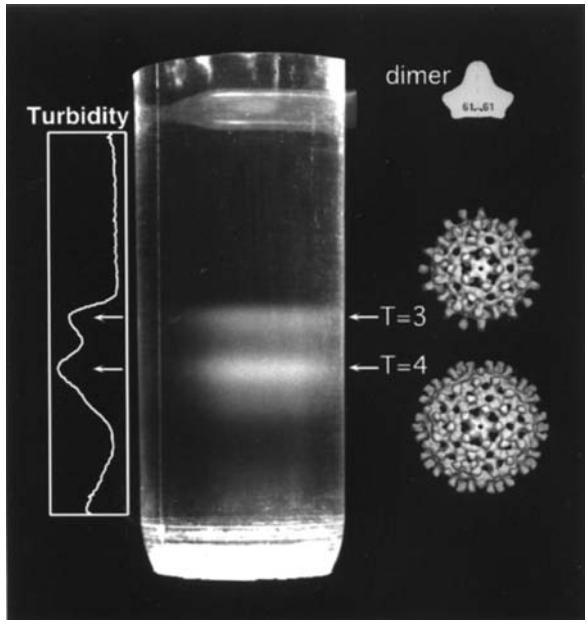

Figure 1
Sucrose gradient showing separation of $T = 3$ and $T = 4$ particles. A shoulder is consistently observed below the $T = 4$ band. The bands are visualized by illumination from below by a fiber-optic light. The turbidity trace (left) is based on analysis of a scanned image of the gradient. A schematic of the capsid-protein dimer with a disulfide crosslink between two cysteine 61 residues and the $T = 3$ and $T = 4$ image reconstructions at 17 Å resolution (Zlotnick *et al.*, 1996) are shown for illustrative purposes. The reconstructions are viewed down the fivefold axes. The scale bar is 100 Å and is only for the reconstructions; the dimer schematic is not to scale.

et al., 1995; Zlotnick *et al.*, 1996, 1997; Böttcher *et al.*, 1997; Conway *et al.*, 1997). The smaller capsids, with a maximum diameter of 318 Å, are assembled from 180 copies of the capsid protein (90 dimers) arranged with $T = 3$ quasi-symmetry (see Caspar & Klug, 1962). The larger capsids consist of 120 dimers arranged with $T = 4$ quasi-symmetry and have a maximum diameter of 348 Å. A 28 Å long spike, formed by the dimer interface, is a dominant feature of the capsid exterior.

The assembly domain has an α-helix-rich fold (Wingfield *et al.*, 1995), unlike the β-barrel capsid proteins observed in most virus structures (Rossmann & Johnson, 1989). Cryo-electron-microscopy image reconstructions, determined to beyond 10 Å resolution, revealed that the dimer-interface spike is formed by a four α-helix bundle (Böttcher *et al.*, 1997; Conway *et al.*, 1997).

A better understanding of the structure of this novel capsid may provide insights into the mechanisms of capsid assembly and polymorphism as well as identifying a target for antiviral therapeutic agents. In this paper, we describe preparative-scale separation of $T = 3$ and $T = 4$ capsids and crystallization of the two forms. Analysis of the crystal packing of the different sizes of the HBV capsid suggests that they use similar lattice contacts.

2. Materials and methods

Dimeric capsid protein can be purified from *E. coli* in the reduced form. HBV capsid protein was expressed and purified from *E. coli* as described (Zlotnick *et al.*, 1996, 1997). Capsid protein (1–2.5 mg ml^{-1}) was stored in 100 m*M* sodium bicarbonate pH 9.5 at 193 K until needed. Capsid-protein dimers were polymerized to the particulate form by 1:1 dilution of a dimer stock with 100 m*M* HEPES pH 7.5, 1 *M* NaCl. To assay for the presence of disulfide bonds, samples which had been pretreated with 5 m*M* iodoacetamide for 20 min to prevent disulfide rearrangement were resolved by SDS–PAGE in the absence of reducing agent. In the absence of reductant, the fraction of disulfide-crosslinked protein, either as dimer or in assembled capsids, slowly increases over time as indicated by the presence of 17 and 34 kDa bands on non-reducing SDS–PAGE (see Fig. 1 in Zlotnick *et al.*, 1997). However, the cysteines are not required for capsid assembly nor for biological activity (Nassal, 1992; Zheng *et al.*, 1992). For this reason, we concentrated our crystallization efforts on the Cp*149 protein which comprises the assembly domain (residues 1–149) with cysteines 48, 61 and 107 mutated to alanine.

Under assembly conditions, Cp*149 dimers polymerize to form a mixture of $T = 3$ (~40%) and $T = 4$ (~60%) capsids (Fig. 1). For comparison, assembly of the wild-type Cp149 without the three cysteine-to-alanine mutations yields ~95% $T = 4$ capsids (Zlotnick *et al.*, 1996). Cp*149 capsids are indistinguishable from capsids of the wild-type sequence in 20 Å resolution image reconstructions (*cf.* Zlotnick *et al.*, 1997).

$T = 3$ and $T = 4$ Cp*149 capsids were separated by velocity sedimentation through sucrose gradients (Fig. 1; 5–30% sucrose containing 100 m*M* HEPES pH 7.5, 300 m*M* NaCl) run at 28000 rev min^{-1} (105000*g*) for 6 h or at 18000 rev min^{-1} (44000*g*) for 14 h at 292 K in an Beckman SW28 rotor (Beckman, Palo Alto, CA). Gradients were formed using a Gradient Master (Biocomp, Fredericton, NB, Canada). Approximately 0.5 ml of freshly assembled capsids, ~2 mg ml^{-1}, was carefully layered onto the gradient. Resolved bands were removed from gradients by side puncture of the centrifuge tube using a syringe with a 20 gauge needle. Based on negative stain EM and analytical ultracentrifugation, the bands have been identified as $T = 3$ and $T = 4$ capsids (Zlotnick *et al.*, 1996). A small amount of protein (<5%) did not assemble. On sucrose gradients prepared with optimal sample loading, it was evident that the $T = 4$ peak consistently had a fast migrating shoulder (Fig. 1). Because of our goal to maximize sample homogeneity, this uncharacterized material was excluded from the pool of $T = 4$ capsids. The final yield of purified $T = 4$ capsid after gradient purification was typically <20% of the initial protein, although ~60% of the protein formed $T = 4$ capsids. The yield of $T = 3$ capsids was ~15% of the initial protein. The purified samples were about 95% homogeneous as determined by analytical ultracentrifugation.

Pooled samples from several gradients were dialyzed against 50 m*M* HEPES pH 7.5, 200 m*M* NaCl and then concentrated approximately tenfold using Ultrafree-15 centrifugal concentrators with a 10 kDa molecular-weight cutoff (Millipore, Bedford, MA). The final concentration step, to at least 10 mg ml^{-1}, utilized Centricon-30 concentrators (Amicon, Beverly, MA). For quality control, samples (0.1 mg ml^{-1} in 0.1 *M* HEPES pH 7.5) were applied to glow-discharged carbon-coated grids, negatively stained with 1% uranyl acetate and viewed with a Zeiss 902 transmission electron microscope (LEO Electron Microscopy, Inc., Thornwood, NY).

$T = 3$ and $T = 4$ capsids were crystallized by the vapor-diffusion method. Initial searches for crystallization conditions were facilitated by kits from Hampton Research

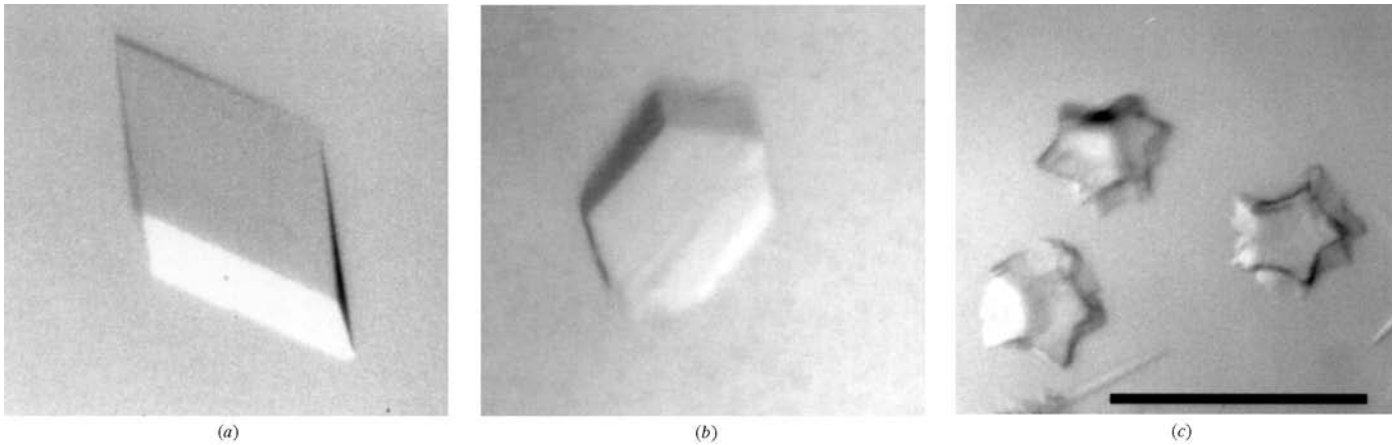

Figure 2
Crystals of HBV Cp*149 capsids. (*a*) Crystals of $T = 4$ capsids, which diffract to ~4 Å resolution. (*b*) Crystals of $T = 3$ capsids, which diffract to ~8 Å resolution. (*c*) Pentagonal quasi-crystals of $T = 3$. No X-ray diffraction has been detected using these small crystals. Scale bar is 0.5 mm.

(Laguna Hills, CA). Crystals of $T = 4$ capsids were grown from 100 m*M* $NaHCO_3$ pH 9.5, 100 m*M* NaCl, 250–350 m*M* KCl, 9.0–9.5% polyethylene glycol monomethyl ether 5000 (PEG–MME) and 10% 2-propanol diluted 1:1 with freshly prepared capsids (10 mg ml^{-1} in 50 m*M* HEPES pH 7.5, 100 m*M* KCl). Crystals grew to maximum dimensions of 0.7 × 0.4 × 0.3 mm. Crystals of $T = 3$ capsids grew in two weeks from 100 m*M* $NaHCO_3$ pH 9.5, 100 m*M* NaCl, 250 m*M* LiCl, 8–8.5% PEG–MME, 10% 2-propanol.

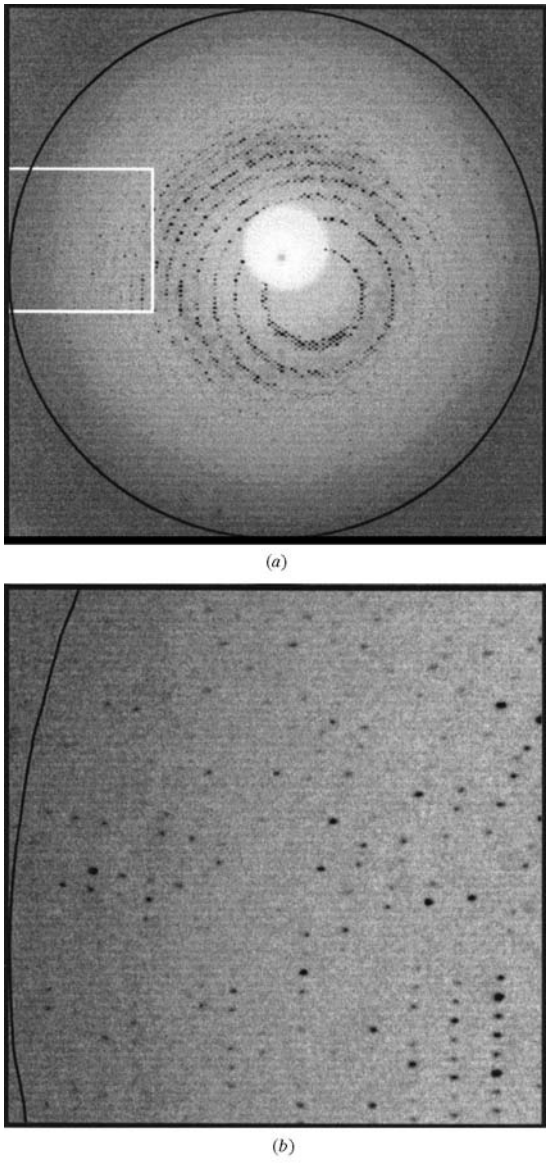

Figure 3
Diffraction pattern from a crystal of $T = 4$ HBV capsids. (*a*) A large inset from a MAR Research 345 diffraction pattern. The edges of the image, nearest the direct beam, are at 4 Å resolution. The highlighted square marks the position of (*b*). (*b*) Inset of the diffraction pattern from 4 to 8 Å resolution. The *d* spacing of the vertical arrayed reflections corresponds to ∼280 Å, *i.e.* half the length of the *a* or *c* spacing. These data were taken at NSLS using beamline X9B with a crystal-to-film distance of 390 mm and an exposure time of 60 s.

High-quality crystals of $T = 4$ Cp*149, grown under conditions that were nearly identical to those of $T = 4$ Cp149 capsids, appeared after about two months and were either rhombohedral or distorted hexagonal plates (Fig. 2*a*). The growth of these crystals was difficult to reproduce and, furthermore, they could not be transferred to synthetic mother liquid containing cryoprotectants without shattering. Crystals of $T = 3$ capsids grew under very similar conditions to those used for $T = 4$ capsids (Fig. 2*b*). In rare cases, using slightly higher LiCl concentrations, crystals of $T = 3$ capsids grew to form five-pointed stars, pentagonal dodecahedra and stellate pentagonal dodecahedra (Fig. 2*c*); pentagonal symmetry is formally forbidden in single crystals but has been observed in infinitely twinned crystals *e.g.* B_6O (Hubert *et al.*, 1998).

3. Results and discussion

Crystals of $T = 4$ capsids of Cp149 were morphologically similar to those of the Cp*149 construct; however, they only diffracted to 7.5 Å resolution. Capillary-mounted crystals of $T = 4$ Cp*149 diffracted to about 4 Å resolution using either 30 s exposures at the National Synchrotron Light Source (NSLS) with a MAR Research 345 detector or 2 h exposures on a Rigaku RU200B rotating-anode X-ray source with an R-AXIS IIc camera (Molecular Structure Corp, Woodlands, TX). Diffraction was only observed for one or two exposures before the diffraction pattern deteriorated (Fig. 3). The φ-angle oscillation was limited to 0.3° to minimize overlapping diffraction maxima. Given the very limited amount of data, unit-cell dimensions of a = 561, b = 330, c = 565 Å, β = 108° (<0.2% distortion) and a probable space group *C*2 were determined using *DENZO* (Otwinowski, 1993). Crystals of $T = 3$ capsids only diffracted to ∼8 Å resolution; a primitive unit cell with a = 293, b = 280, c = 875 Å, $\alpha = \beta = \gamma = 90°$ (<0.1% distortion) was determined with rotating-anode data using *DENZO*. Packing constraints based on particle size indicate that both $T = 3$ and $T = 4$ unit cells contain four capsids. The unit-cell dimensions of the $T = 4$ crystal are consistent with a pseudo-rhombohedral packing arrangement (see Natarajan & Johnson, 1999) based on cryo-EM-determined dimensions for the capsids, *i.e.* the diameter is between 290 and 350 Å, depending on contact with surface protrusions. A rhombohedral angle is close to the 63.4° between icosahedral fivefold axes, consistent with a role for the icosahedral fivefold in particle packing (see Fry *et al.*, 1996; Natarajan & Johnson, 1999). A reasonable, though insufficiently constrained, packing arrangement for the $T = 3$ particles would place particles at approximate fractional coordinates of (0, 0, 1/8), (0, 1/2, 3/8), (0, 0, 5/8) and (0, 0, 7/8). This creates a diamond-shaped layer (consistent with the symmetry constraints of space groups $P2_1$, $P22_12$ and $P2_12_12$) with an ∼66° angle between capsids. As with the $T = 4$ particles, this packing arrangement suggests that icosahedral fivefolds play a role in lattice contacts. The similarities in crystallization conditions and the presence of twinned crystals with pentagonal symmetry are consistent with this conjecture.

Icosahedral fivefolds often have a role in virus crystal contacts (Natarajan & Johnson, 1999, and references therein). Image reconstructions of $T = 3$ and $T = 4$ capsids (Fig. 1) show that their icosahedral fivefold vertices are nearly identical (Zlotnick *et al.*, 1996); this is the only region of identity in the quaternary structure of the capsids (*cf.* the image reconstructions in Fig. 1; Zlotnick *et al.*, 1996). The similarities in crystallization conditions for the two forms suggest that similar lattice contacts are made. Fivefold vertices are further implicated in crystal-lattice contacts by the growth of pentagonally symmetrical pseudo- or quasi-crystals of $T = 3$ capsids. Though not exclusive, packing arrangements for both crystals are proposed where lattice contacts are consistent with icosahedral geometry. The angle between adjacent icosahedral fivefolds is 63.4°, compared with 66.1 and 60.3° angles between capsids in the proposed packing of $T = 3$ and $T = 4$ unit cells, respectively.

The determination of the structure of $T = 4$ HBV capsids is being pursued using crystals prepared as described in this paper. The 9 Å resolution cryo-electron-microscopy structure (Conway *et al.*, 1997) is suitable for a preliminary molecular-replacement phasing model. The phases can be extended to the 4 Å resolution limit of the data by taking advantage of the 60-fold non-crystallographic symmetry (Fry *et al.*, 1996). The

only real hurdle to overcome in this structure determination is growing a large number of these crystals, which are difficult to reproduce. Furthermore, the improved preparation and separation of HBV capsids should facilitate improving the crystallization conditions of the $T = 3$ form.

This research was carried out in part at the National Synchrotron Light Source, Brookhaven National Laboratory, which is supported by the US Department of Energy, Division of Materials Sciences and Division of Chemical Sciences. Dr Szbyszek Dauter provided invaluable support at Brookhaven. We thank Dr Craig Hyde for the use of his X-ray equipment. AZ was supported by a NRC-NIAMS post-doctoral fellowship.

References

Bartenschlager, R. & Schaller, H. (1992). *EMBO J.* **11**, 3413–3420.
Birnbaum, F. & Nassal, M. (1990). *J. Virol.* **64**, 3319–3330.
Blumberg, B. S. (1997). *Proc. Natl Acad. Sci. USA*, **94**, 7121–7125.
Böttcher, B., Wynne, S. A. & Crowther, R. A. (1997). *Nature (London)*, **386**, 88–91.
Caspar, D. L. D. & Klug, A. (1962). *Cold Spring Harbor Symp. Quant. Biol.* **27**, 1–24.
Cohen, B. J. & Richmond, J. E. (1982). *Nature (London)*, **296**, 677–679.
Conway, J. F., Cheng, N., Zlotnick, A., Wingfield, P. T., Stahl, S. J. & Steven, A C. (1997). *Nature (London)*, **386**, 91–94.
Crowther, R. A., Kiselev, N. A., Böttcher, B., Berriman, J. A., Borisova., G. P., Ose, V. & Pumpens, P. (1994). *Cell*, **77**, 943–950.
Fry, E., Logan, D. & Stuart, D. (1996). *Methods Mol. Biol.* **56**, 319–363.
Hubert, H., Devouard, B., Garvie, L. A. J., O'Keefe, M., Buseck, P. R., Petuskey, W. T. & McMillen, P. F. (1998). *Nature (London)*, **391**, 376–378.
Kenney, J. M., von Bonsdorff, C. H., Nassal, M. & Fuller, S. D. (1995). *Structure*, **3**, 1009–1019.
Milich, D. R., McLachlan, A., Stahl, S., Wingfield, P., Thornton, G. B., Hughes, J. L. & Jones, J. E. (1988). *J. Immunol.* **141**, 3617–3624.
Nassal, M. (1992). *Virology*, **190**, 499–505.
Natarajan, P. & Johnson, J. E. (1999). In the press.
Otwinowski, Z. (1993). *Proceedings of the CCP4 Study Weekend. Data Collection and Processing*, edited by L. Sawyer, N. Isaacs & S. Bailey, pp. 56–62. Warrington: Daresbury Laboratory.
Pasek, M., Goto, T., Gilbert, W., Zink, B., Schaller, H., MacKay, P., Leadbetter, G. & Murray, K. (1979). *Nature (London)*, **282**, 575–579.
Rossmann, M. G. & Johnson, J. E. (1989). *Annu. Rev. Biochem.* **58**, 533–573.
Stahl, S., MacKay, P., Magazin, M., Bruce, S. A. & Murray, K. (1982). *Proc. Natl Acad. Sci. USA*, **79**, 1606–1610.
Summers, J. & Mason, W. S. (1982). *Cell*, **29**, 403–415.
Wingfield, P. T., Stahl, S. J., Williams, R. W. & Steven, A. C. (1995). *Biochemistry*, **34**, 4919–4932.
Zheng, J., Schodel, F. & Peterson, D. L. (1992). *J. Biol. Chem.* **267**, 9422–9429.
Zlotnick, A., Cheng, N., Conway, J. F., Booy, F. P., Steven, A. C., Stahl, S. J. & Wingfield, P. T. (1996). *Biochemistry*, **35**, 7412–7421.
Zlotnick, A., Cheng, N., Stahl, S. J., Conway, J. F., Steven, A. C. & Wingfield, P. T. (1997). *Proc. Natl Acad. Sci. USA*, **94**, 9556–9561.